

Space observations of inland water bodies show rapid surface warming since 1985

Philipp Schneider¹ and Simon J. Hook¹

Received 11 August 2010; revised 24 September 2010; accepted 15 October 2010; published 24 November 2010.

[1] Surface temperatures were extracted from nighttime thermal infrared imagery of 167 large inland water bodies distributed worldwide beginning in 1985 for the months July through September and January through March. Results indicate that the mean nighttime surface water temperature has been rapidly warming for the period 1985–2009 with an average rate of $0.045 \pm 0.011^\circ\text{C yr}^{-1}$ and rates as high as $0.10 \pm 0.01^\circ\text{C yr}^{-1}$. Worldwide the data show far greater warming in the mid- and high latitudes of the northern hemisphere than in low latitudes and the southern hemisphere. The analysis provides a new independent data source for assessing the impact of climate change throughout the world and indicates that water bodies in some regions warm faster than regional air temperature. The data have not been homogenized into a single unified inland water surface temperature dataset, instead the data from each satellite instrument have been treated separately and cross compared. Future work will focus on developing a single unified dataset which may improve uncertainties from any inter-satellite biases. **Citation:** Schneider, P., and S. J. Hook (2010), Space observations of inland water bodies show rapid surface warming since 1985, *Geophys. Res. Lett.*, 37, L22405, doi:10.1029/2010GL045059.

1. Introduction

[2] Near surface air temperature measurements have been widely used to characterize recent warming trends over land, and *in situ* measurements in conjunction with satellite data have been used to characterize similar trends over the oceans [Intergovernmental Panel on Climate Change, 2007; Smith and Reynolds, 2005; Hansen et al., 2006]. Over land, these analyses are based primarily on different subsets of the same raw air temperature dataset. In contrast to the land surface, the surface temperature and associated trends of inland water bodies can be accurately measured with thermal infrared data from satellite instruments since the emissivity of water is well known [Hook et al., 2003; Schneider et al., 2009]. The temperatures of large inland water bodies are good indicators of climate change [Livingstone, 2003; Austin and Colman, 2008; Williamson et al., 2009] and have been used for climate change studies [Livingstone, 2003; Verburg et al., 2003; Vollmer et al., 2005; Coats et al., 2006; Austin and Colman, 2008; Quayle et al., 2002]. However, such studies are relatively few in number and limited to water bodies with long, regular time series of *in*

situ measurements. Such data are scarce and largely geographically restricted to North America and Europe.

[3] Satellite data have the potential to provide a continuous worldwide record of surface temperatures of inland water bodies extending back to the early 1980s. These data have been collected by a variety of sensors including the Advanced Very High Resolution Radiometers (AVHRR) instrument series and the Along Track Scanning Radiometer series of instruments consisting of ATSR-1, ATSR-2, and AATSR (henceforth jointly referred to as ATSR). AVHRR and ATSR data have been available since 1978 and 1991, respectively. These sensors have been used to determine changes in global ocean surface temperature from 1985 to 2000 with trends between $0.009^\circ\text{C yr}^{-1}$ and $0.018^\circ\text{C yr}^{-1}$ [Lawrence et al., 2004; Good et al., 2007], but only recently have such data been used to determine the trends of inland water bodies [Schneider et al., 2009]. We provide results from utilizing these data to examine temperature trends for inland water bodies worldwide.

2. Data and Methodology

2.1. Study Sites

[4] An initial selection of water bodies used in the study was made based on a minimum water surface area of 500 km^2 utilizing data from the Global Lakes and Wetlands Database (GLWD) [Lehner and Döll, 2004]. From the resulting 364 potential sites, 167 were subsequently selected based on the existence of an approximately $10 \text{ km} \times 10 \text{ km}$ pure water area in order to ensure that temperature retrievals could be extracted without contamination from shoreline pixels. A latitude and longitude pair for data extraction was then manually chosen for each study site at the point maximizing the distance from any shoreline (including islands) to avoid any possible contamination by the land surface. The analysis assumes that the selected area of the site is representative of the entire water body with respect to long-term trends. This assumption is reasonable based on comparisons at different locations in the Great Lakes.

2.2. Remote Sensing Data

[5] The ATSR data used in the study were acquired between 1991 and 2009. A 3×3 pixel array (nominal pixel size 1 km^2 at center of nadir swath and $1.5 \text{ km} \times 2.0 \text{ km}$ at center of forward swath) was extracted around the location of each study site for each nighttime satellite overpass. Any cloudy pixels were masked from the time series of top-of-atmosphere brightness temperatures using a subset of the cloud tests provided with the ATSR product and an additional spatial homogeneity test that excluded any arrays where the standard deviation of the 3×3 pixel array was

¹Jet Propulsion Laboratory, California Institute of Technology, Pasadena, California, USA.

greater than 0.5°C. Skin surface water temperatures were computed from the top-of-atmosphere brightness temperatures using the dual-view operational split-window coefficients for ATSR [Merchant *et al.*, 1999] and subsequently converted to bulk water temperatures using sensor-specific correction factors obtained from the Great Lakes validation.

[6] The AVHRR data used in the study were acquired between 1985 and 2009 and were taken from the Version 5 product of AVHRR Pathfinder [Kilpatrick *et al.*, 2001]. This joint NASA/NOAA 4 km resolution global reprocessing of the AVHRR dataset includes twice daily temperatures of large inland water bodies worldwide. For the location selected at each study site the temperature value of a single pixel was extracted from each nighttime image. Only nighttime data were used to minimize bias due to orbital drift of the sensors. A subset of the cloud tests provided with the AVHRR Pathfinder product was used to identify and exclude the majority of cloudy pixels. Any additional pixels acquired at zenith angles greater than 45 degrees, and with standard deviations greater than 0.5°C were discarded. The Pathfinder dataset has been validated against comprehensive *in situ* data [Kearns *et al.*, 2000; Marullo *et al.*, 2007] over the oceans and was validated in this study against *in situ* data at the Great Lakes. The cloud-free AVHRR and ATSR values were then merged into a single dataset to maximize the sampling frequency.

2.3. In Situ Data

[7] Nine National Data Buoy Center (NDBC) buoys on the Great Lakes were used for validation, which have been providing hourly samples of bulk water temperature at depths of 0.6 m to 1 m since the early 1980s. The buoys used were 45001, 45004 and 45006 (Lake Superior), 45002 and 45007 (Lake Michigan), 45003 and 45008 (Lake Huron), 45005 (Lake Erie), and 45012 (Lake Ontario). This data set has been used in earlier studies to determine summertime trends in surface water temperature [Austin and Colman, 2007] and was used to validate the time series and long-term trends derived from the satellite data in this study. Any year when the buoy data contained measurement gaps in the averaging period was excluded (typically two years per buoy).

2.4. Trend Estimates

[8] Computing an annual average water temperature from thermal infrared data would be very valuable but due to prolonged winter ice cover and/or cloudy periods this is only possible at very few sites. Instead, a seasonal average temperature is generally used. Previously the mean surface water temperature of the three month period between July and September (JAS) has been used to represent summertime temperature [Austin and Colman, 2007; Schneider *et al.*, 2009]. This metric works well in the mid- and high latitudes of the northern hemisphere where it generally coincides with ice-free water bodies and the most cloud-free days. For this global study we modified the approach such that in the southern hemisphere the mean was computed over the months of January through March (JFM). To avoid the cloudy wet season in the tropics, a dry-season metric was used, i.e., the JFM mean was computed for latitudes between the equator and 23.5°N and the JAS mean was computed for latitudes between the equator and 23.5°S.

[9] The satellite observations are not always distributed evenly over the averaging period due to cloud cover. In order to avoid sampling bias, a robust locally weighted regression smoothing (LOWESS) approach [Cleveland, 1979] was used on a year-by-year basis. This technique allows the construction of a temporally continuous surface temperature estimate that is robust against outliers in the data and was used to compute the JAS and JFM means for each year of available data. The seasonal average was only computed if the averaging period included at least 20 temperature retrievals. Ordinary linear regression analysis was then applied to the JAS and JFM means to help identify any trends in the data. Non-parametric trend estimation techniques provided very similar results, so only linear regression was further considered. Each time series was also visually inspected to ensure there were no artifacts or processing errors. Trends were only computed if at least 15 valid seasonal means out of a possible 25 years were available.

[10] The uncertainty for each trend estimate was computed using Monte Carlo analysis in order to incorporate the individual uncertainty for the data point of each single year and to derive a more realistic estimate of the overall trend uncertainty by incorporating interannual autocorrelation of the errors. The seasonal average of each year was simulated 10,000 times as an independent, normally distributed random variable with a year-dependent error derived from the validation against the NDBC buoys. For all 10,000 simulations a linear least squares model was fitted and overall uncertainty was computed as the standard deviation of the slopes computed from all realizations, and trend significance was estimated as the median p-value of the distribution.

3. Results and Discussion

3.1. Validation

[11] Differences in calibration between sensors or orbital drift can introduce artificial biases in estimated trends. Several steps were undertaken to ensure neither of these effects were present in the results. Firstly, in order to check the calibration, individual retrievals from all three ATSR sensors were validated against *in situ* observations at the Great Lakes (Figure S1 of the auxiliary material).¹ The results for ATSR-1, ATSR-2, and AATSR indicate biases of 0.09°C, 0.02°C, and -0.04°C, and standard deviations of 0.55°C, 0.33°C, and 0.44°C, respectively, with no observable drift of sensor retrievals. It should be noted here that due to the small magnitude of the observed biases, no specific correction of ATSR inter-sensor bias was carried out. However, while small, such biases can affect the accuracy of the trends reported here and future studies using a homogenized satellite record may improve trend accuracy.

[12] No validation of individual retrievals was possible for AVHRR Pathfinder data due to the lack of a specific observation time given in the product, but validation of AVHRR JAS means indicates a bias of 0.15°C with a standard deviation of 0.31°C and root mean squared error (RMSE) of 0.53°C. Secondly, a time series of annual biases was produced (Figure S2 of the auxiliary material) for both AVHRR and ATSR and a linear regression analysis showed no significant trend in the errors (rates were found

¹Auxiliary materials are available in the HTML. doi:10.1029/2010GL045059.

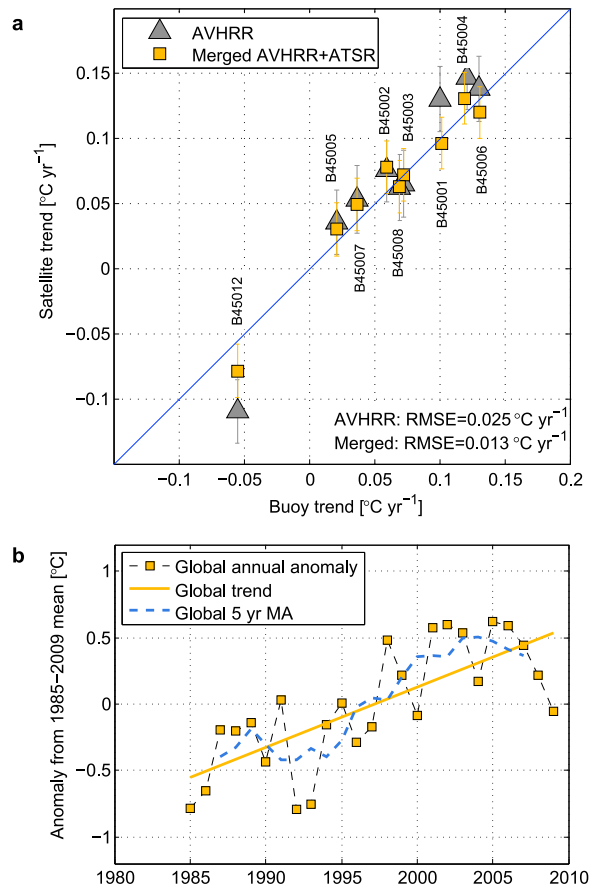


Figure 1. (a) Scatterplot of trends derived from AVHRR and the merged AVHRR/ATSR data set against trends computed from eight buoys at the Great Lakes. Error bars are standard deviation of slope in linear regression. (b) Anomaly time series of the mean average over all study sites worldwide. Anomaly computed as the difference from the 1985 to 2009 mean for each water body. MA represents the moving average. All sites weighted equally, thus the signal is dominated by the mid-latitudes of the northern hemisphere.

to be $0.006^{\circ}\text{C yr}^{-1}$ and $-0.004^{\circ}\text{C yr}^{-1}$, respectively, with $p > 0.2$ in both cases), indicating that calibration drift does not adversely affect the trends obtained from the data. The trend in the AVHRR errors over the Great Lake region does not appear to display a strong bias due to aerosols from the 1991 Mount Pinatubo eruption, however other regions might be more susceptible to this effect and this needs to be taken into account in the interpretation of the results. Previous studies have shown that long-term trends from both ATSR and AVHRR Pathfinder are capable of calculating long-term temperature trends that are not adversely affected by calibration drift [Lawrence *et al.*, 2004; Good *et al.*, 2007].

[13] In order to further confirm that the surface temperature trends observed with *in situ* water measurements could also be measured from satellite data and are not affected by calibration issues, we computed trends of the mean water surface temperature for the July through September (JAS) period from nine Great Lakes buoys beginning in 1985. These data were then compared with corresponding trends derived from satellite data. Figure 1a shows the trends from the *in situ* data plotted against AVHRR only data and merged AVHRR and ATSR data. The trends from AVHRR

show good agreement with the trends obtained from the *in situ* data. Most AVHRR data points fall close to the 1:1 line, with the errors ranging from $-0.054^{\circ}\text{C yr}^{-1}$ to $0.03^{\circ}\text{C yr}^{-1}$, a mean bias of $0.005^{\circ}\text{C yr}^{-1}$, and a standard deviation and RMSE of $0.025^{\circ}\text{C yr}^{-1}$. Figure 1a also shows the trends computed from both ATSR and AVHRR data. The errors in trends range between $-0.023^{\circ}\text{C yr}^{-1}$ and $0.019^{\circ}\text{C yr}^{-1}$, with a mean bias of $0.0004^{\circ}\text{C yr}^{-1}$ and a standard deviation and RMSE of $0.013^{\circ}\text{C yr}^{-1}$. Both the bias and standard deviation are reduced in the merged dataset, which is used in the remainder of the study. In addition, assuming a normal distribution, these results indicate that seasonal averages of AVHRR-only data can be used to reliably ($p < 0.05$) infer positive non-zero trends in excess of $0.047^{\circ}\text{C yr}^{-1}$, whereas the merged data set can do so for non-zero trends in excess of $0.023^{\circ}\text{C yr}^{-1}$. It should be noted that this validation and the associated error estimates were obtained at large “sea-like” lakes at modest elevation, for which the used SST products are likely to provide the best results. While the data have also been validated with good results at elevations of around 2000 m (Lake Tahoe [Hook *et al.*, 2003; Schneider *et al.*, 2009] and Crater Lake, CA), some very high elevation sites on the Tibetan Plateau and in the Andes may have higher uncertainties associated with the absolute water temperature.

3.2. Worldwide Trends

[14] Seasonal means were computed at all 167 inland water bodies used in the study. Linear trends were then computed at 113 water bodies that had a minimum of 15 valid annual seasonal means. Overall, rates of change varied between $-0.018 \pm 0.014^{\circ}\text{C yr}^{-1}$ and $0.13 \pm 0.011^{\circ}\text{C yr}^{-1}$. Forty-one sites showed a significant trend with $p < 0.05$ (sixty-one sites when using a standard parametric p-value rather than the median p-value derived from Monte Carlo analysis). The average rate of change over all sites was $0.045 \pm 0.011^{\circ}\text{C yr}^{-1}$ and the average rate of change of sites with significant trends ($p < 0.05$) was $0.065 \pm 0.011^{\circ}\text{C yr}^{-1}$.

[15] Figure 2a summarizes the trends for all sites. Several consistent spatial patterns emerge from the data set. The largest and most consistent area of rapid warming with trends of approximately $0.08^{\circ}\text{C yr}^{-1}$ occurs in Northern Europe and includes Lake Vänern, Lake Onega, and Lake Ladoga. The trends weaken slightly towards southeastern Europe ($\sim 0.06^{\circ}\text{C yr}^{-1}$). Around the Black Sea and the Caspian Sea, as well as in the area of Kazakhstan the trends are weaker and average around $0.04^{\circ}\text{C yr}^{-1}$ to $0.05^{\circ}\text{C yr}^{-1}$. Even further east, in Siberia, Mongolia, and northern China, the trends increase slightly to rates of $0.05^{\circ}\text{C yr}^{-1}$ to $0.07^{\circ}\text{C yr}^{-1}$. In North America, trends in the southwest U.S. average around $0.07^{\circ}\text{C yr}^{-1}$ and in the Great Lakes region average around $0.05^{\circ}\text{C yr}^{-1}$ to $0.06^{\circ}\text{C yr}^{-1}$. In the tropics, most lakes exhibited weak trends with rates of $0.025^{\circ}\text{C yr}^{-1}$ on average. All the sites in the mid-latitudes of the southern hemisphere showed insignificant trends with an average rate of $0.012^{\circ}\text{C yr}^{-1}$.

[16] The primary factors of the lake heat budget are net radiation, sensible heat flux, and latent heat flux. Here we compare lake temperature trends with those of surface air temperature. In addition to being ubiquitously observed, surface air temperature influences both sensible and to some extent latent heat exchange. Figure 2b shows a map of global JAS surface air temperature change from GISTEMP [Hansen *et al.*, 2006], allowing a direct comparison of

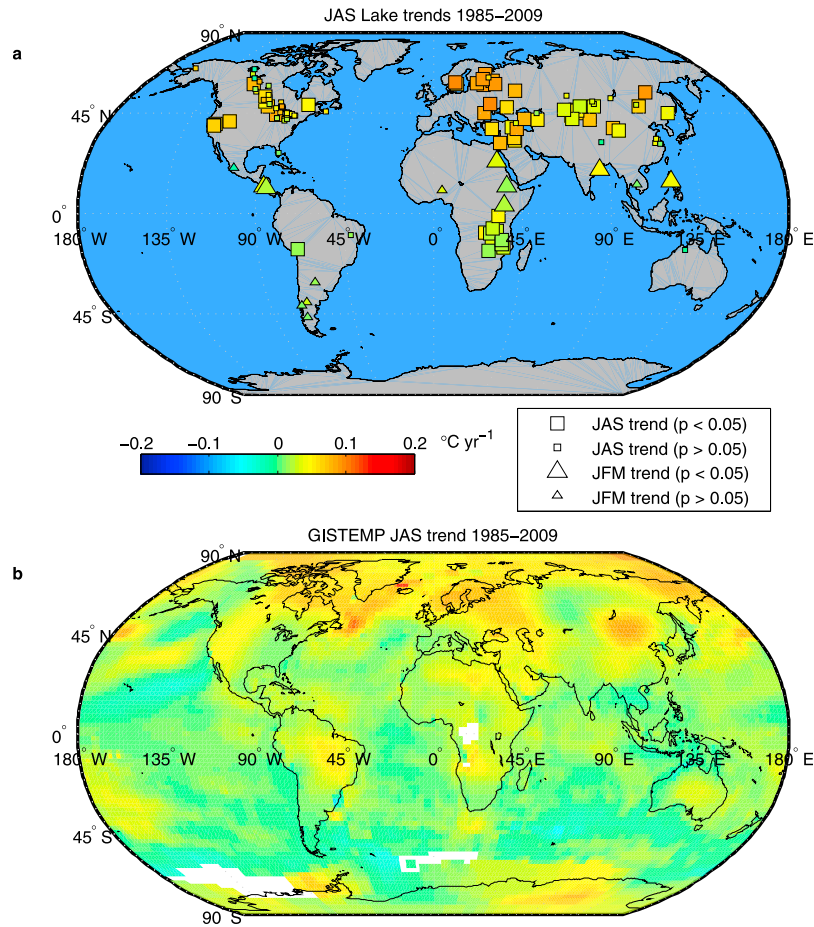


Figure 2. (a) Worldwide trends in nighttime lake surface temperature derived from satellite data. JAS trends were computed for all sites located north of 23.5°N and between 0° and 23.5°S, while JFM trends were computed for all sites located south of 23.5°S and between 0° and 23.5°N. (b) Corresponding map of worldwide JAS trends in surface air temperature from GISTEMP [Hansen *et al.*, 2006]. JFM GISTEMP map is not shown due to the small number of JFM sites.

spatial patterns between the JAS inland water and JAS air temperature trends (the JFM GISTEMP map is not shown due to the small number of stations for which JFM means were computed). The spatial patterns between the two datasets show good agreement. In particular over Eurasia the strong warming in northern and eastern Europe as well as the hotspot in southern Siberia and Mongolia are apparent. In North America, the warming trend around the Great Lakes region is not as apparent in the air temperature trends map. The warming in the southwestern U.S. corresponds fairly well with a ridge of strong warming in the GISTEMP JAS map. The inland water trends in the low latitudes are weaker and similar to those found in the GISTEMP analysis for the same region. While the spatial patterns of water surface and air temperature trends generally agree, there are areas (e. g. around the Great Lakes and in Northern Europe) in which the water bodies appear to warm more rapidly than the surrounding air temperature. This effect has been documented previously in studies using satellite [Schneider *et al.*, 2009] and *in situ* measurements [Austin and Colman, 2007]. The latter authors suggest that the more rapid water temperature trends are due to decreasing winter ice cover and the associated lower albedo. Apart from an investigation of similarities in spatial patterns, a quantitative analysis of differences in water and air temperature trends revealed a

correlation between the two parameters of $\rho = 0.42$. This relatively weak relationship indicates that changes in insolation, ice cover, and other factors are important contributing factors in explaining the spatial patterns found.

[17] Figure 1b shows the overall mean anomaly of JAS/JFM nighttime inland water surface temperature over all study sites as compared to the 1985–2009 mean. Features such as the 1992/1993 cooling due to aerosols from the Mt. Pinatubo eruption and the warm anomaly in 1998 caused by the strong El Niño event are clearly visible in the time series. From the mean data set we found an overall linear warming trend of $0.045 \pm 0.011^\circ\text{C yr}^{-1}$ ($p < 0.001$). This trend is dominated by the large number of water bodies in the mid-latitudes of the northern hemisphere. A mean trend over all sites with northern and southern hemisphere ($0.052^\circ\text{C yr}^{-1}$ and $0.023^\circ\text{C yr}^{-1}$, respectively) weighted equally was determined as $0.037 \pm 0.011^\circ\text{C yr}^{-1}$ and this rate is very similar to global trends derived from land-surface air temperature data for the same period [Smith and Reynolds, 2005; Hansen *et al.*, 2006].

4. Conclusion

[18] Nighttime satellite imagery was used to study recent trends in the surface temperatures of large inland water

bodies and to obtain an independent data set of temperature change over land. Initially the trends determined from the satellite data were validated against the trends from nine buoys in the Great Lakes. The satellite-derived trends for the 1985 to 2009 period showed good agreement with the trends from the *in situ* data with an RMSE of $0.013^{\circ}\text{C yr}^{-1}$. The same methodology was then applied to large inland water bodies worldwide, and significant warming trends were found at 41 of the locations with the inland water body temperature trends showing agreement with trends from independent air temperature observations. For certain regions such as the Great Lakes and Northern Europe, however, we found that water temperature increases more rapidly than regional air temperature. The results suggest that climate strongly influences the surface temperature of inland water bodies worldwide.

[19] **Acknowledgments.** The research described here was carried out at the Jet Propulsion Laboratory, California Institute of Technology, under a contract with the National Aeronautics and Space Administration. The authors wish to acknowledge funding by the NASA Earth Observing System, support from ESA, and contributions by Robert Radocinski, Gary Corlett, Glynn Hulley, and Geoff Schladow.

References

- Austin, J. A., and S. M. Colman (2007), Lake Superior summer water temperatures are increasing more rapidly than regional air temperatures: A positive ice-albedo feedback, *Geophys. Res. Lett.*, *34*, L06604, doi:10.1029/2006GL029021.
- Austin, J., and S. Colman (2008), A century of temperature variability in Lake Superior, *Limnol. Oceanogr.*, *53*(6), 2724–2730.
- Cleveland, W. (1979), Robust locally weighted regression and smoothing scatterplots, *J. Am. Stat. Assoc.*, *74*(368), 829–836, doi:10.2307/2286407.
- Coats, R., J. Perez-Losada, G. Schladow, R. Richards, and C. Goldman (2006), The Warming of Lake Tahoe, *Clim. Change*, *76*(1–2), 121–148, doi:10.1007/s10584-005-9006-1.
- Good, S. A., G. K. Corlett, J. J. Remedios, E. J. Noyes, and D. T. Llewellyn-Jones (2007), The global trend in sea surface temperature from 20 years of advanced very high resolution radiometer data, *J. Clim.*, *20*(7), 1255–1264, doi:10.1175/JCLI4049.1.
- Hansen, J., M. Sato, R. Ruedy, K. Lo, D. Lea, and M. Medina-Elizade (2006), Global temperature change, *Proc. Natl. Acad. Sci. U. S. A.*, *103*(39), 14,288–14,293, doi:10.1073/pnas.0606291103.
- Hook, S. J., F. J. Prata, R. E. Alley, A. Abtahi, R. C. Richards, S. G. Schladow, and S. O. Palmarsson (2003), Retrieval of lake bulk and skin temperatures using Along-Track Scanning Radiometer (ATSR-2) data: A case study using Lake Tahoe, California, *J. Atmos. Oceanic Technol.*, *20*(4), 534–548, doi:10.1175/1520-0426(2003)20<534:ROL-BAS>2.0.CO;2.
- Intergovernmental Panel on Climate Change (2007), *Climate change 2007: The Physical Science Basis. Contribution of Working Group I to the Fourth Assessment Report of the Intergovernmental Panel on Climate Change*, edited by S. Solomon et al., Cambridge Univ. Press, Cambridge, U. K.
- Kearns, E. J., J. A. Hanafin, R. H. Evans, P. J. Minnett, and O. B. Brown (2000), An independent assessment of Pathfinder AVHRR sea surface temperature accuracy using the Marine Atmosphere Emitted Radiance Interferometer (MAERI), *Bull. Am. Meteorol. Soc.*, *81*(7), 1525–1536, doi:10.1175/1520-0477(2000)081<1525:AIAOPA>2.3.CO;2.
- Kilpatrick, K. A., G. P. Podesta, and R. Evans (2001), Overview of the NOAA/NASA advanced very high resolution radiometer Pathfinder algorithm for sea surface temperature and associated matchup database, *J. Geophys. Res.*, *106*(C5), 9179–9197, doi:10.1029/1999JC000065.
- Lawrence, S. P., D. T. Llewellyn-Jones, and S. J. Smith (2004), The measurement of climate change using data from the Advanced Very High Resolution and Along Track Scanning Radiometers, *J. Geophys. Res.*, *109*, C08017, doi:10.1029/2003JC002104.
- Lehner, B., and P. Döll (2004), Development and validation of a global database of lakes, reservoirs and wetlands, *J. Hydrol.*, *296*, 1–22, doi:10.1016/j.jhydrol.2004.03.028.
- Livingstone, D. (2003), Impact of secular climate change on the thermal structure of a large temperate central European lake, *Clim. Change*, *57*(1–2), 205–225, doi:10.1023/A:1022119503144.
- Marullo, S., B. Buongiorno Nardelli, M. Guarracino, and R. Santoleri (2007), Observing the Mediterranean Sea from space: 21 years of Pathfinder-AVHRR sea surface temperatures (1985 to 2005): Re-analysis and validation, *Ocean Sci.*, *3*, 299–310, doi:10.5194/os-3-299-2007.
- Merchant, C., A. Harris, M. Murray, and A. Zavody (1999), Toward the elimination of bias in satellite retrievals of sea surface temperature: 1. Theory, modeling and interalgorithm comparison, *J. Geophys. Res.*, *104*(C10), 23,565–23,578, doi:10.1029/1999JC900105.
- Quayle, W., L. Peck, H. Peat, J. Ellis-Evans, and P. Harrigan (2002), Extreme responses to climate change in Antarctic lakes, *Science*, *295*, 645, doi:10.1126/science.1064074.
- Schneider, P., S. J. Hook, R. G. Radocinski, G. K. Corlett, G. C. Hulley, S. G. Schladow, and T. E. Steissberg (2009), Satellite observations indicate rapid warming trend for lakes in California and Nevada, *Geophys. Res. Lett.*, *36*, L22402, doi:10.1029/2009GL040846.
- Smith, T. M., and R. W. Reynolds (2005), A global merged land-air-sea surface temperature reconstruction based on historical observations (1880–1997), *J. Clim.*, *18*(12), 2021–2036, doi:10.1175/JCLI3362.1.
- Verburg, P., R. E. Hecky, and H. Kling (2003), Ecological consequences of a century of warming in Lake Tanganyika, *Science*, *301*, 505–507, doi:10.1126/science.1084846.
- Vollmer, M. J., H. A. Bootsma, R. E. Hecky, G. Patterson, J. D. Halfman, J. M. Edmond, D. H. Eccles, and R. F. Weiss (2005), Deep-water warming trend in Lake Malawi, East Africa, *Limnol. Oceanogr.*, *50*(2), 727–732, doi:10.4319/lo.2005.50.2.0727.
- Williamson, C., J. Saros, and D. Schindler (2009), Sentinels of change, *Science*, *323*, 887–888, doi:10.1126/science.1169443.

S. J. Hook and P. Schneider, Jet Propulsion Laboratory, California Institute of Technology, MS 183-501, 4800 Oak Grove Dr., Pasadena, CA 91109, USA. (simon.j.hook@jpl.nasa.gov)